Extended data

Chemotherapy may facilitate colorectal cancer metastasis through vessel formation by upregulating G-CSF

Yueping Zhan et, al.

Table 1

IF antibodies:

Confocal	Name	Imformation
CD31/P-STAT3	CD31	R，77699S，CST/M
	P-STAT3	M，4113S，CST
CD31/SELE	CD31	R，77699S，CST
	SELE	M，BBA16，R&D
CD31/SELP	CD31	R，77699S，CST
	SELP	sc-19672，Santa Cruz
CD34		R，ab81289，abcam
VEGFR2		R，ab39638，abcam

Fig. S1 Chemotherapy promote lung metastasis and the formation of vessels. A, Study design for b–d (n = 5 for BALB/C mice injected with-FU, CPT-11, OXA, or blank controls, three days later CT26-luc cells were injected by tail vein injection. B, Luciferase-based bioluminescence imaging on experimental lung metastasis of indicated mice treated with the MTD of 5-FU, CPT-11, OXA, or blank controls. C, Representative pictures and quantitative results of hematoxylin and eosin (H&E) staining of lung sections from indicated mice in A. Left panel: H&E images; right panel: the quantitative data for lung metastatic. D, The microvascular density was assayed by immunofluorescence for $CD31^+$ cells (Left). The percent of $CD31^+$ tumor area and p-$STAT3^+$ area was averaged from 10 random area (2 random area from each mice, n=5). Scale bars, 30 μm.

Statistical significance calculated using one-way ANOVA with Dunnett's test. Data represented as mean ± s.d.

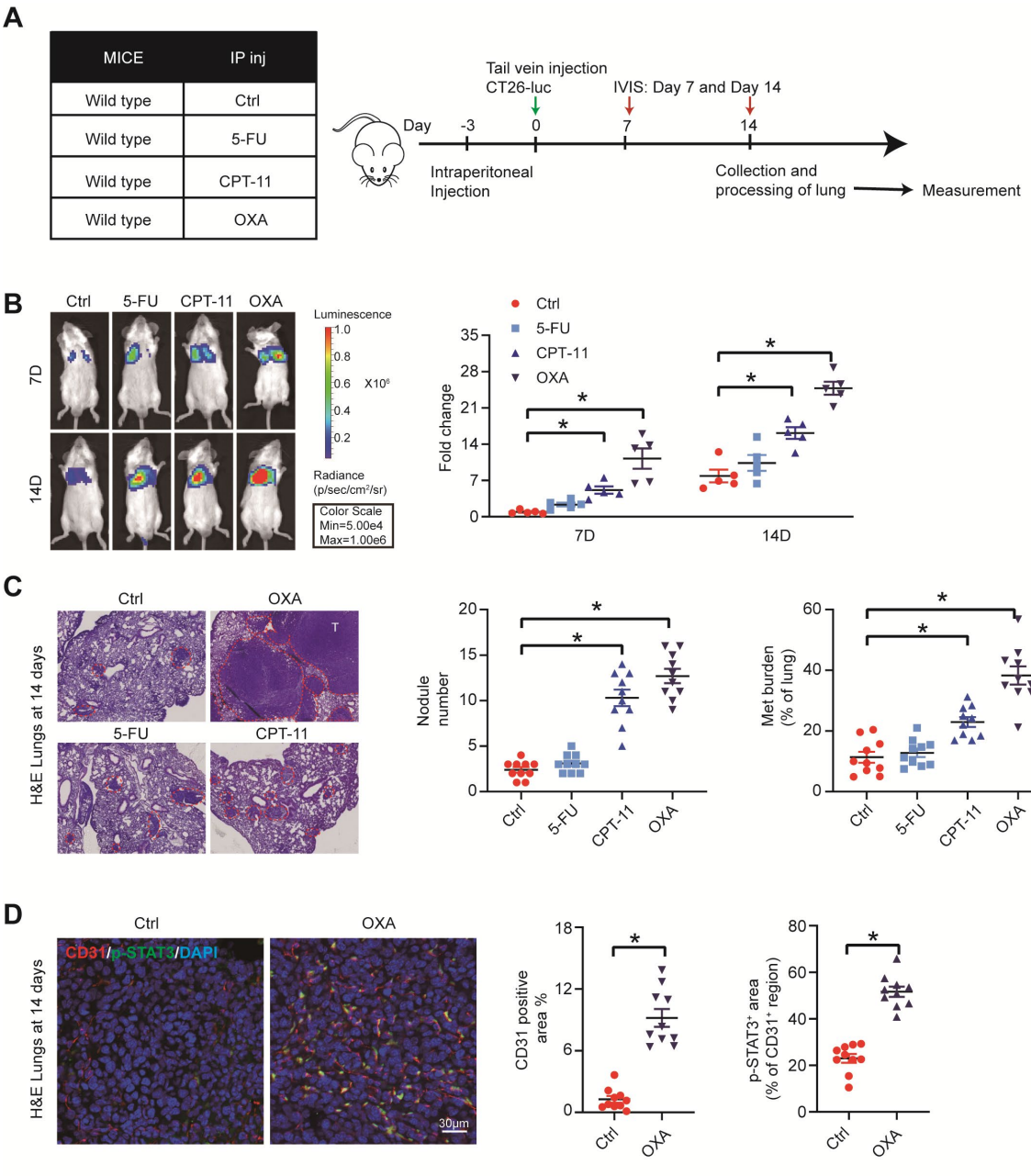

Fig. S2 Chemotherapy promote the immunosuppression by the infiltration of MDSCs. A. The infiltration of MDSCs detected by immunofluorescence. The number of MDSCs was averaged from 10 random area (2 random area from each mice, n=5). Scale bars, 30 μm. Statistical significance calculated using one-

way ANOVA with Dunnett's test. Data represented as mean ± s.d. B, C, The infiltration of CD4+T and CD8+T cells were detected by IHC. The number of MDSCs was averaged from 5 random area (1 random area from each mice, n=5). Scale bars, 30 μm. Statistical significance calculated using one-way ANOVA with Dunnett's test. Data represented as mean ± s.d.

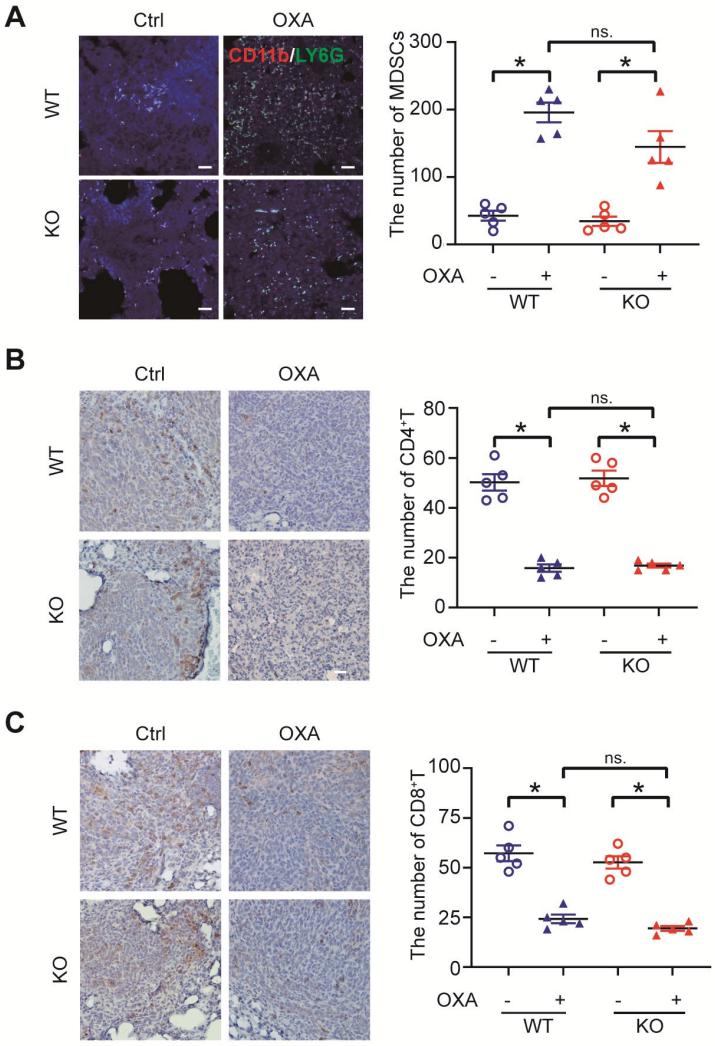

Fig. S3 Mobilization EPCs and MDSCs to mediate vasculogenesis and immunosuppression after chemotherapy. A, Study design for B-D, n=3. B, C, The mobilization of EPCs from bone marrow to plasma detected by FACS. D, The mobilization of MDSCs from bone marrow to plasma detected by FACS. Statistical significance calculated using one-way ANOVA with Dunnett's test. Data represented as mean ± s.d.

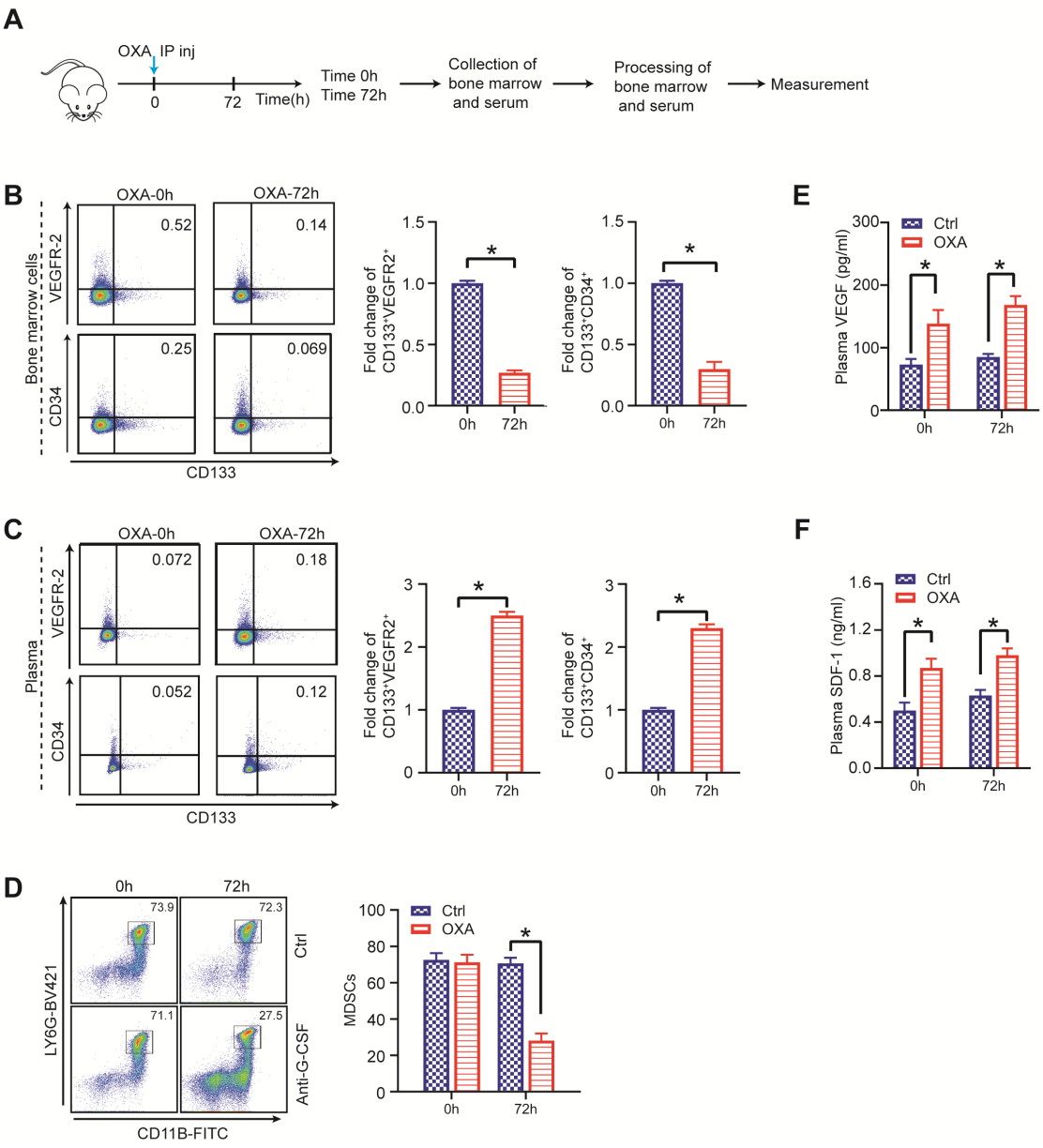

Fig. S4 G-CSF doesn't affect the proliferation and migration of HUVECs. A, The proliferation of HUVEC detected by CCK8. B, C, The migration of HUVEC evaluated by Wound Healing and Transwell test. Statistical significance calculated using one-way ANOVA with Dunnett's test. Data representative of Three independent experiments. Data represented as mean ± s.d.

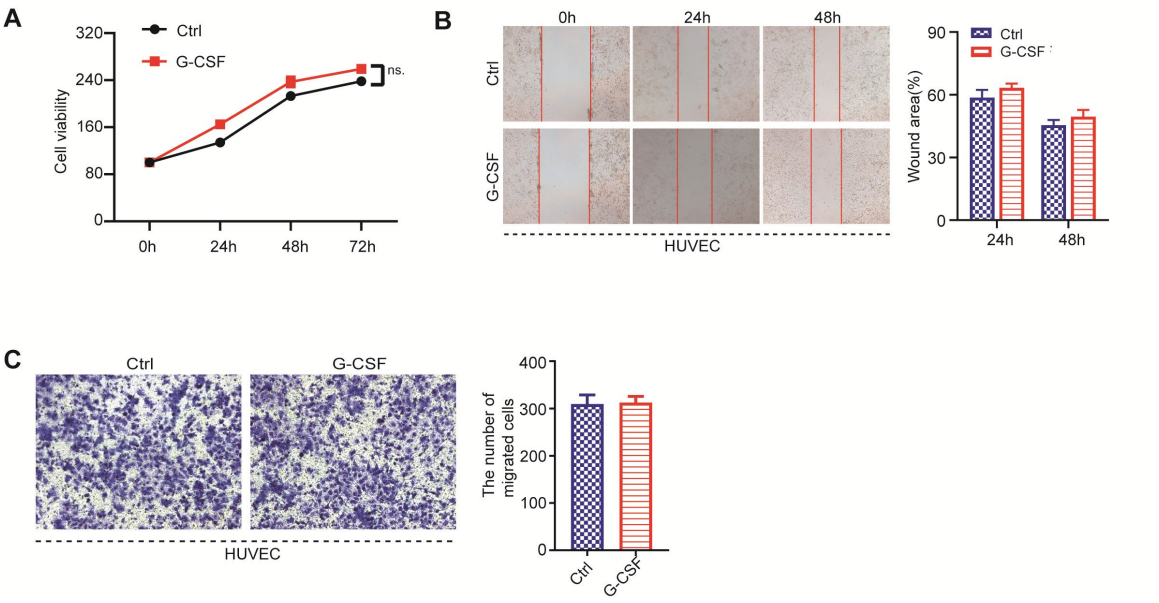

Fig. S5 Anti-G-CSF reduced the chemotherapy-induced lung metastasis by modulate vascular adhesion. A, Study design for B–J (n = 5 for BALB/C mice injected OXA, two hours later i.p. injected with anti G-CSF or IgG; three days later MC38-luc cells were injected by tail vein injection). B, Luciferase-based bioluminescence imaging on indicated mice in A. For each group, five mice were used for quantification. C, The metastasis of lung imaging on indicated mice in A. D, Representative pictures and quantitative results of hematoxylin and eosin (H&E) staining of lung sections from indicated mice in A. Left panel: H&E images; right panel: the quantitative data for lung metastatic. E, Images of CD31 in tumor metastasis site (2 random area from each mice, n=5). Scale bars, 30 μm. F, The p-STAT3^{+} of CD31^{+} cells were assayed by immunofluorescence (Left). The percent of p-STAT3^{+} area was averaged from 10 random area (2 random area from each mice, n=5). Scale bars, 30 μm. G-J, The expression of SELE, MDSCs, CD34 and VEGFR2 detected by immunofluorescence (2 random area from each mice, n=5). Scale bars, 30 μm. Statistical significance calculated using one-way ANOVA with Dunnett's test. Data represented as mean ± s.d.

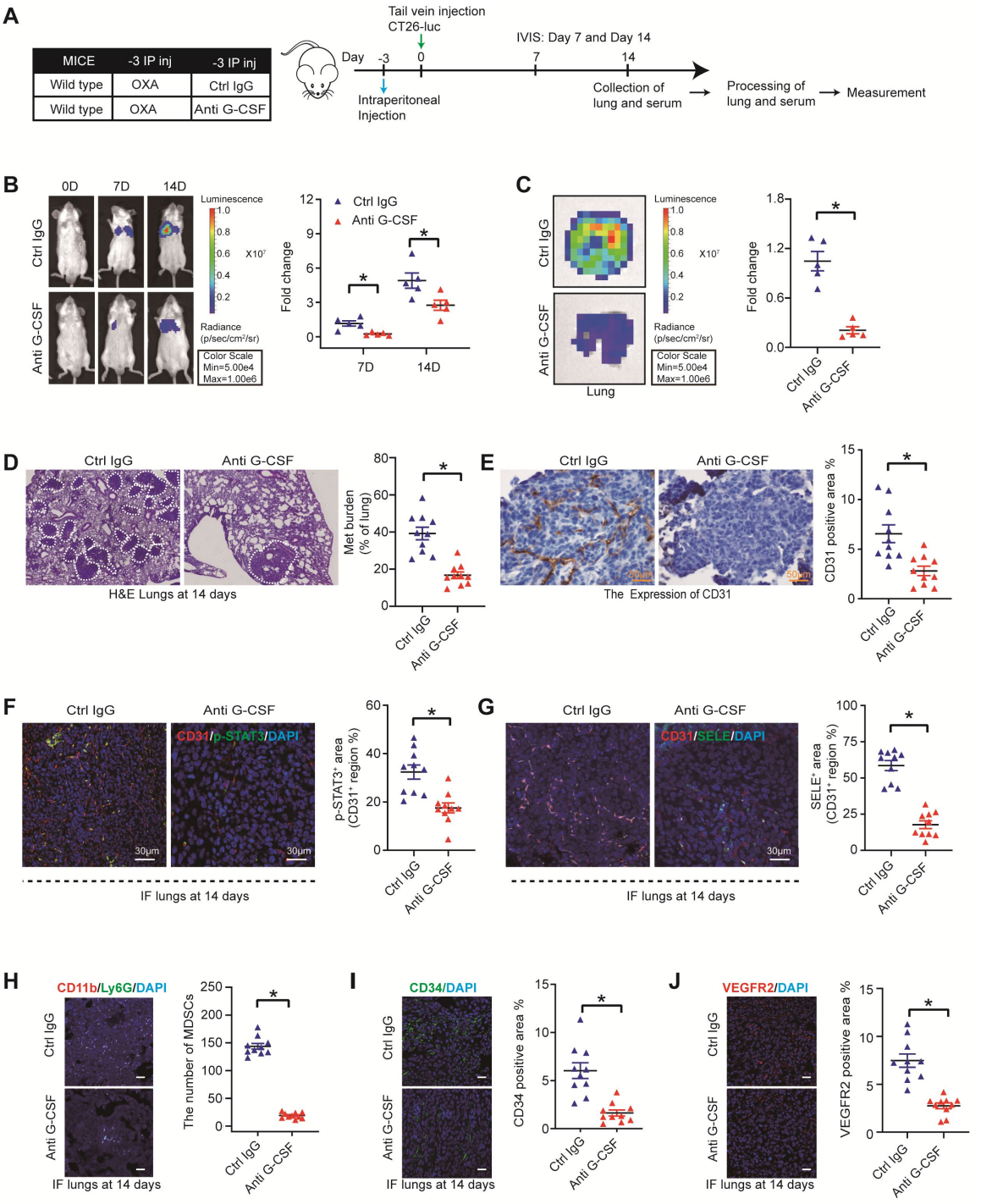

Fig S6 Anti-G-CSF reduced the infiltration of CD4+ T and CD8+t cells after chemotherapy. A, B The infiltration of CD4+T and CD8+T cells were detected by IHC. The number of MDSCs was averaged from 5 random area (1 random area from each mice, n=5). Scale bars, 30 μm. Statistical significance calculated using one-way ANOVA with Dunnett's test. Data represented as mean ± s.d.

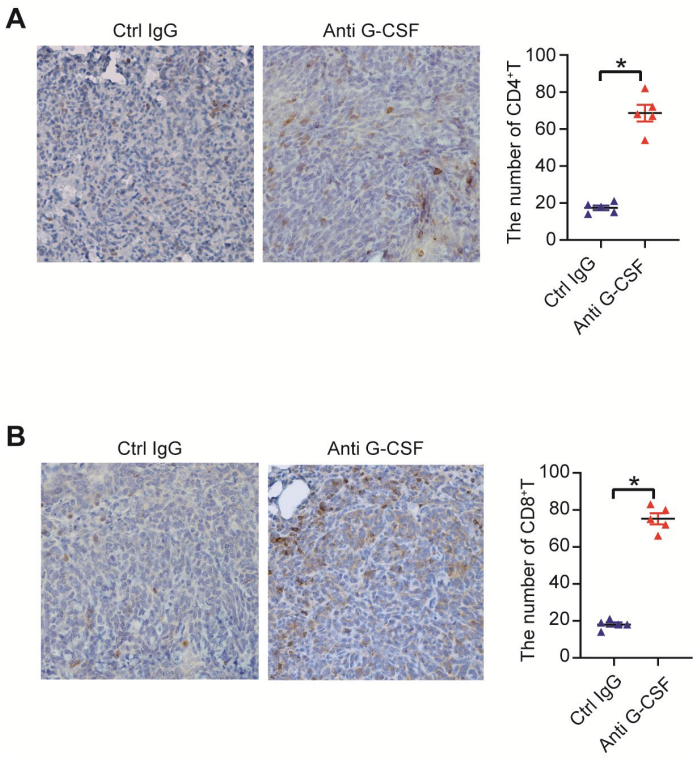

Fig. S7 Chemotherapy promote lung metastasis and the formation of vessels. A, Study design for b–d (n = 5 for BALB/C mice injected with OXA, or blank controls, three days later Lewis-luc cells were injected by tail vein injection. B, Luciferase-based bioluminescence imaging on experimental lung metastasis of indicated mice in A. C, Representative pictures and quantitative results of hematoxylin and eosin (H&E) staining of lung sections from indicated mice in A. Left panel: H&E images; right panel: the quantitative data for lung metastatic. D, The microvascular density was assayed by immunofluorescence for $CD31^+$ cells (Left). The percent of $CD31^+$ tumor area and p-$STAT3^+$ area was averaged from 5 random area (1 random area from each mice, n=5). Scale bars, 30 μm. E, Study design for b–d (n = 5 for C57Bl/6 mice injected with OXA, or blank controls, three days later B16F10-luc cells were injected by tail vein injection. F, G The metastasis of lung in the chemotherapy treated mice. H, The microvascular density was assayed by immunofluorescence for $CD31^+$ cells (Left). The percent of $CD31^+$ tumor area and p-$STAT3^+$ area was averaged from 5 random area (1 random area from each mice, n=5). Scale bars, 30 μm. Statistical significance

calculated using one-way ANOVA with Dunnett's test. Data represented as mean ± s.d.